Proceedings of the 2nd International Conference on Fluid Flow and Thermal Science (ICFFTS'21)
~~Seoul, South Korea~~ Virtual Conference - November 24- 26, 2021
Paper No. 108
DOI: 10.11159/icffts21.108

Finite-time Lyapunov Exponent analysis used on a free-surface flow problem solved by Smoothed Particle Hydrodynamics

Petr Jančík[1], Tomáš Hyhlík[1]
[1]My Institute/CompanyDepartment of Fluid Mechanics and Thermodynamics, Faculty of Mechanical Engineering, Czech Technical University in Prague
Technická 4, 160 00, Prague 6, Czech Republic

Abstract **-** This paper presents a combination of a free-surface flow problem solution using Smoothed Particle Hydrodynamics (SPH) with an analysis of the results by Finite-Time Lyapunov Exponents method (FTLE). Both these methods originate from the Lagrangian de-scription and work with continuum particles, which makes their combination relatively straightforward. FTLE is a method used primarily for the identification of coherent structures, for example, vortices. However, this work focuses mainly on how FTLE can de-scribe the evolution of free surfaces; their emerging and vanishing. There are two variants of FTLE: forward-in-time and backward-in-time. Both variants give different information about the flow and by their combination, we can get an interesting picture revealing some hidden characteristics that are not apparent at first sight.

Keywords**:** Smoothed Particle Hydrodynamics, Finite-Time Lyapunov Exponents, free-surface, Lagrangian Coherent Structures

1. Introduction

Various structures in fluid flow fields, such as vortices and eddies, are in the scope of researchers for many decades. Their analysis using primary quantities, such as velocity, cannot provide us a full understanding of these phenomena. Some methods for their identification and quantification have been proposed, Q-criterion [1], Δ-criterion [2], or λ2-criterion [3], to name just the most widely used. The named methods work with the velocity field. This is convenient because velocity fields are naturally widespread outputs of practically all numerical or experimental methods in fluid dynamics.

However, this approach is not the only one possible. Another possibility is to use a material description and analyse the trajectories of continuum particles. In this context, we talk about so-called Lagrangian Coherent Structures (LCSs). Simply put, LCSs are surfaces in the flow field that are impenetrable by materials. The fluid bounded by these structures share either the same origin or fate. A strong argument for Lagrangian approach is that methods based on velocity gradient field are not objective, meaning they give different results in different coordinate systems [4]. Lagrangian methods also offer a deeper understanding of a flow.

One way to identify LCSs is Finite-Time Lyapunov Exponents (FTLE) method. It has been shown that ridges formed by mutually repulsing or attracting particles are LCSs and the method was applied to experimental and numerical data [5]. However, particle trajectories usually have to be extracted from the velocity field first, and FTLE evaluation follows. It is computationally expensive [6]. Thus, it seems reasonable to use FTLE with a method that works with particles directly like SPH.

Sun et al. developed two algorithms for the evaluation of FTLE within SPH framework: through particle position and through time integration [7]. The algorithms were also implemented on GPUs for fast computations [8].

This paper focuses on the implementation of a previously published method of FTLE working with data from SPH. The used variant of SPH method is briefly described. FTLE is described in greater detail. Then the method was used on a simple free-surface problem and the results are analysed and discussed. In contrast to usually analysed problems like vortex shedding or turbulence is the current field aperiodic, and it is also solved as inviscid (there is only artificial numerical viscosity). It appears that not only vortices might be identified but the analysis can give us a better insight into phenomena like mixing and free-surface evolution. Possible future steps in the work are discussed as well.

2. Methods

2.1. Smoothed Particle Hydrodynamics

Smoothed Particle Hydrodynamics (SPH) is a numerical method originating from the material description of continuum. It is especially suitable for the solution of free-surface flows and transient problems. Fluid is discretized in the form of particles of constant mass, and the motion of these particles is given by the governing equations

$$\frac{\mathrm{D}\rho_i}{\mathrm{D}t} = \rho_i \sum_j \frac{m_j}{\rho_j} (\mathbf{v}_i - \mathbf{v}_j) \cdot \nabla W_{ij} \tag{1}$$

$$\frac{\mathrm{D}\mathbf{v}_i}{\mathrm{D}t} = -\sum_j m_j \left(\frac{p_i}{\rho_i^2} + \frac{p_j}{\rho_j^2} + \Pi_{ij} \right) \nabla W_{ij} + \mathbf{g} \tag{2}$$

where indices i and j denote particles, W is so-called smoothing function, and Π stands for the artificial viscosity term. Other symbols follow the usual notation: t is time, ρ is density, m is mass, $\mathbf{v}$ is velocity, and $\mathbf{g}$ is gravity acceleration.

The relation between density and pressure is given by the equation of state

$$p = c^2(\rho - \rho_0) \tag{3}$$

where c is the numerical speed of sound and ρ_0 is the fluid density at zero gauge pressure [9]. The numerical speed of sound is chosen according to the solved problem to keep the variation in liquid density under 1%.

In this work, a truncated Gaussian smoothing function [9] was used and Monaghan's artificial viscosity [10]. Wall boundary conditions are modelled as free-slip using virtual particles according to [11]. The author of this paper used a virtually identical solution method in his previous work [12], [13]. For more details about the method see, e.g., [9].

2.2. Finite-Time Lyapunov Exponents

There are two variants of FTLE: forward-in-time (FTLE^+) and backward-in-time (FTLE^-). These identify mutually attracted and repulsed particles, respectively. Both are used in this work. The method that uses the particle positions proposed in [7] was employed.

Let's define a material point vector $\mathbf{X}$ in its initial time t_0. This material point changes its position to $\mathbf{x}$ at the current time t. The current position is a function of the initial position and time, i.e., $\mathbf{x} = \mathbf{x}(\mathbf{X}, t)$. We can define the deformation gradient tensor for the continuum motion between time instances t_0 and t

$$\mathbf{F}_{t_0}^{t}(\vec{X}) = \frac{\partial \mathbf{x}}{\partial \mathbf{X}} \tag{4}$$

and then forward-in-time Right-Cauchy-Green strain tensor

$$\mathbf{C}_{t_0}^{t}(\mathbf{X}) = \left[\mathbf{F}_{t_0}^{t}(\mathbf{X})\right]^T \mathbf{F}_{t_0}^{t}(\mathbf{X}) \tag{5}$$

Since this tensor is symmetric and positive definite, its eigenvalues are real and positive. Moreover, it can be shown that it is linked only to a stretching deformation of the continuum and not its rotation and the eigenvalues have the meaning of stretching in the directions of eigenvectors. Therefore, the maximum eigenvalue $\Lambda_{\max}$ can be used as a measure of the stretching deformation.

The forward-in-time Right-Cauchy-Green strain tensor from Eq. 5 can describe any deformation between two different configurations, not only from the initial to the current. From the kinematic point of view, there is also no difference between time marching forward and backward. We will use these properties when defining FTLE formulas.

To define FTLE$^+$, let's set another time instance t_f which is in the future relative to the current time t. This variant can be written

$$\lambda_t^{t_f}(\mathbf{x}) = \frac{1}{|t_f - t|} \ln \sqrt{\Lambda_{max}\left[\mathrm{C}_t^{t_f}(\mathbf{x})\right]} \tag{6}$$

FTLE$^-$ is defined

$$\lambda_t^{t_0}(\mathbf{x}) = \frac{1}{|t_0 - t|} \ln \sqrt{\Lambda_{max}\left[\mathrm{C}_t^{t_0}(\mathbf{x})\right]}\,. \tag{7}$$

Note that now t_0 does not necessarily denote the initial configuration but any time instance before t.

We need to evaluate the deformation gradient tensor $\mathbf{F}$ defined by Eq. 4 in SPH framework. It can be done using the formula

$$\mathbf{F}_{t_0}^t(\mathbf{X}_i) = \sum_j (\mathbf{x}_j - \mathbf{x}_i) \otimes \mathbf{L}(\mathbf{X}_i) \nabla W\left(|\mathbf{X}_j - \mathbf{X}_i|\right) \left(\frac{m_j}{\rho_j}\right)_{t_0} \tag{8}$$

where $\mathbf{L}(\mathbf{X}_i)$ is the smoothing function consistency improving tensor and it is calculated

$$\mathbf{L}(\mathbf{X}_i) = \left[\sum_j (\mathbf{X}_j - \mathbf{X}_i) \otimes \nabla W\left(|\mathbf{X}_j - \mathbf{X}_i|\right) \left(\frac{m_j}{\rho_j}\right)_{t_0}\right]^{-1} \tag{9}$$

To get FTLE according to Eqs. 6 and 7, we change the arguments in Eqs. 8 and 9. For FTLE+, we evaluate the deformation gradient from t to t_f ($\mathbf{F}_t^{t_f}$), and for backward-in-time from t to t_0 ($\mathbf{F}_t^{t_0}$).

FTLE$^-$ can be evaluated parallel to the solution because we know the particle positions in the past. Clearly, this is not possible for FTLE$^+$ because the future configuration is not calculated yet. In this work, FTLE was computed and analysed in postprocessing using MATLAB.

3. Problem Definition

The method is demonstrated on a variation of a simple dam-break problem in two dimensions. There are two columns of liquid (one higher and one shorter) which start collapsing due to gravity. The resulting surges meet in the middle part of the tank, resulting in violent flow patterns. The initial configuration is depicted in Fig. 1.

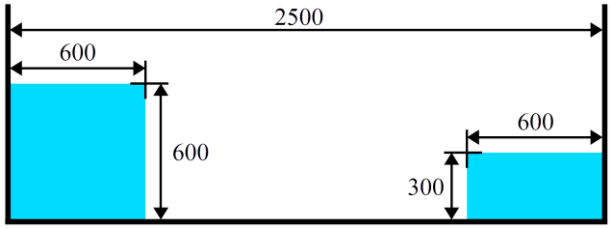

Fig. 1: Scheme of the problem. Dimensions in millimetres.

Reference liquid density ρ_0 is $1000\ \mathrm{kg \cdot m^{-3}}$. There are 60 000 liquid particles, and 4 seconds are simulated. It was chosen $t_0 = 0$ s and $t_f = 4$ s.

4. Results and Discussion

The results are presented in the form of FTLE fields for a chosen set of time instances. $FTLE^+$ is in Fig. 2, $FTLE^-$ 3. Distinct features of the flow are further commented and marked in the figures. $FTLE^+$ is not defined at $t = t_f$ because it is not defined there and for a similar reason $FTLE^-$ is not defined for $t = t_0$. Note that the color scales are different for various times to visualize the fields correctly. This is due to the aperiodic nature of the analyzed field. Moreover, the results become meaningless close to the mentioned definition limits.

In Fig. 2a there is the initial configuration. In both liquid columns there are distinct areas with low values of $FTLE^+$. In the higher column approximately in the centre, and in the lower column in its bottom centre. These spots are parts of the liquid that stay together throughout the whole simulation. They move with the flow and get deformed but not mixed with liquid from other parts. No other structures are visible in this configuration.

Fig. 2b and Fig. 3a depict the same time instance shortly after the waves hit one another. A massive jet of fluid is about to impact the fluid layer beneath on the right-hand side of the tank, while a rolling wave emerges at the position x=1.5 m and starts moving leftwards. In $FTLE^+$, the two spots in the middle of each column are joined together and some ridges that will form future structures become apparent. There is a very distinct ridge in $FTLE^-$. This ridge clearly separates the fluid from the two initial liquid columns. This structure remains dominant for the rest of the simulation.

Fig. 2c and Fig. 3b capture a very violent situation after the jet hit the fluid layer on the right, and the impact of the rolling wave moving left resulted in a sequence of rolling waves and jets. In both pictures, two large counter-rotating structures resulting from the jet impact are visible. One in the bottom right corner of the tank (I) and the other one about 0.7 m to the right (II). The most distinct structures in the left are two (counter-rotating again) eddies (III and IV). In $FTLE^+$, there is a visible difference between the vortices. While the right one (III) is bounded by a ridge that separates it from the rest of the fluid, the left one (IV) forms an unrolling spiral. Worth noticing is also the boundary between fluid from different columns in $FTLE^-$. Most of the liquid from the right column remains in the right and partially mixes with the other fluid. However, a thin layer near the bottom reached eddy III and it transports it further to the left.

Fig. 2d and Fig. 3c depict a situation when a series of jets and rolling waves propagate from the left wall back to the right. The surface is relatively calm in the right part of the tank. A relatively large vortices I and II split into two smaller eddies (I to Ia and Ib, and II to IIa and IIb). These vortices are noticeable in both $FTLE^+$ and $FTLE^-$ fields. The same applies for vortex III. However, vortex IV is no longer apparent in $FTLE^+$ because its rotation stopped. In $FTLE^-$ we can see a stretching deformation of the material that formed eddy IV. There is another vortex in the bottom left corner of the tank (V) that emerged as a consequence of a wave impacting the left wall. The thin layer of liquid from the lower column commented in the previous paragraph evolved as it wound up further on eddy III.

In Fig. 3d, we can see the fluid in the end of the simulation. The waves reached the right wall and the overall motion gets mitigated by the artificial viscosity. Towards the end of the simulation, we are limited to $FTLE^-$ field because of the lower information value of $FTLE^+$ fields for t and t_f being too close values. Some structures highlighted in the previous paragraphs are still noticeable even though majority of the vortices ceased to exist. There are only parcels of fluid that once formed vortices. Probably the best example is vortex IV which got stretched into a very thin layer. This process started also for vortex III. Eddies Ia and IIb are no longer visible at all. On the other hand, a new vortex (VI) appeared as a result of one of the rolling waves. Worth noticing are also the large areas of low $FTLE^-$ values in the middle of the tank. These are formed by the same liquid particles as the low $FTLE^-$ spots in Fig. 2a. The distinct ridge separating the bigger and the smaller parcel separates liquid from the higher and the lower column. Fluid in these areas changed its position and got deformed but did not mix with other fluid (as already mentioned in the second paragraph of this section)

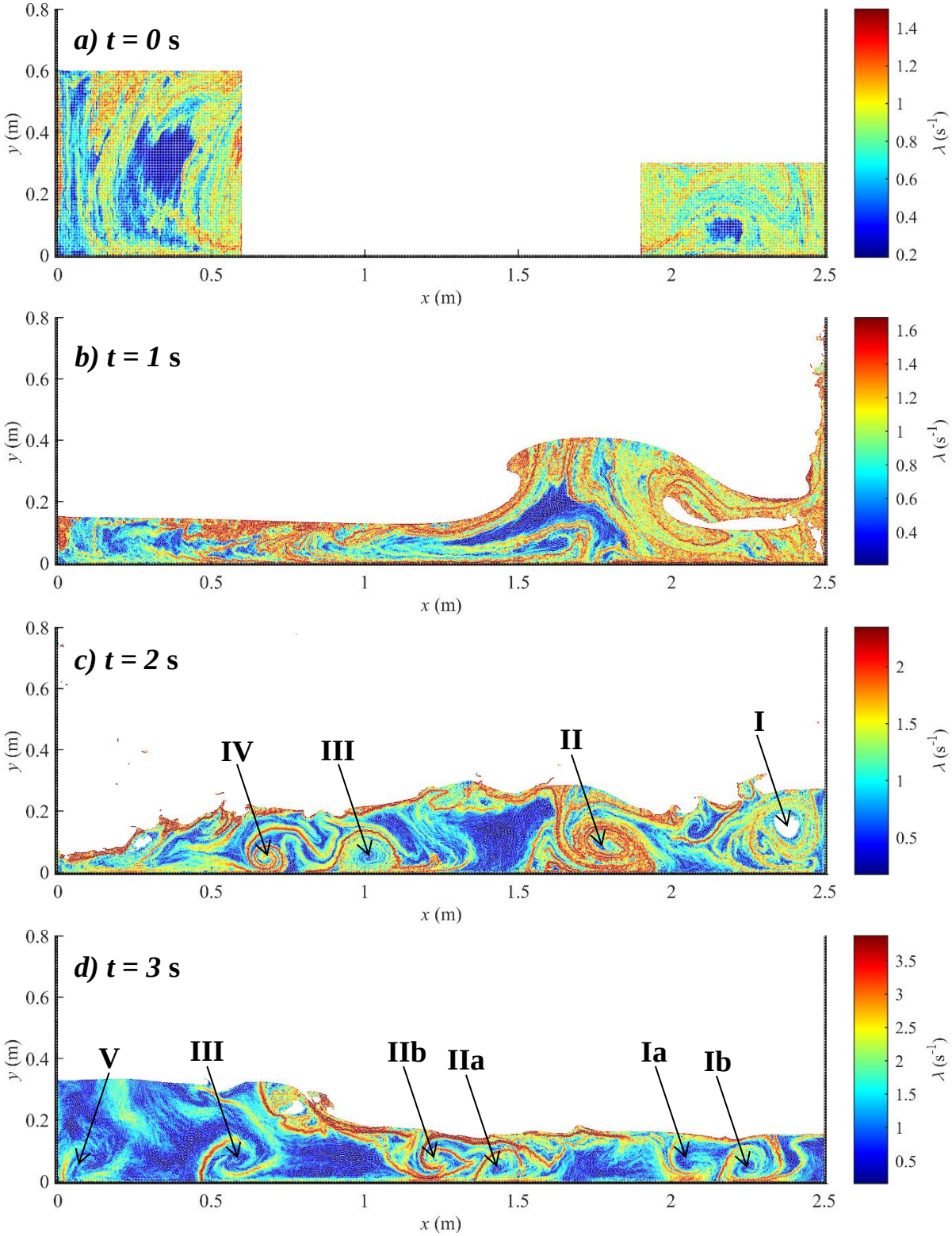

Fig. 2: FTLE^{+} for chosen time instances.

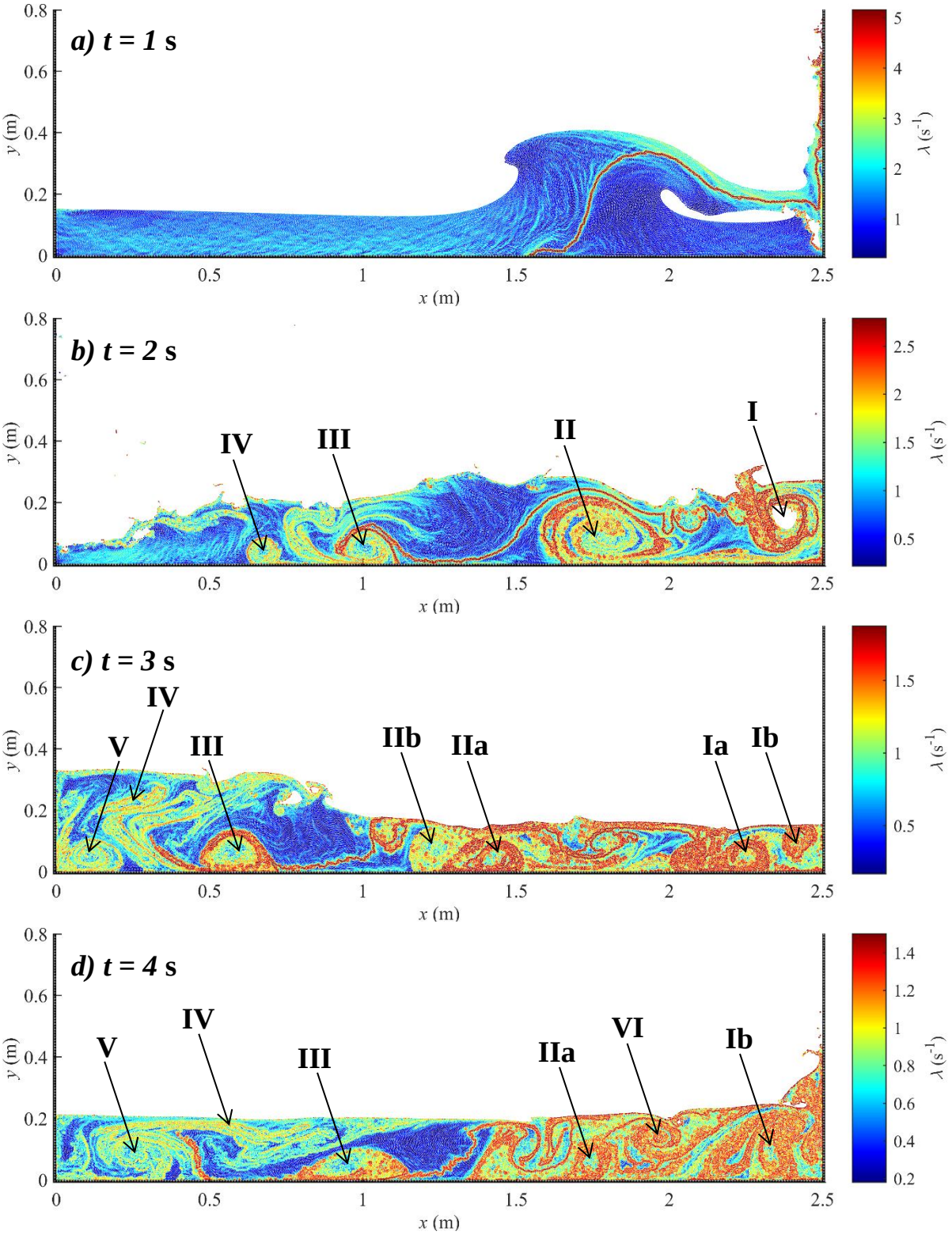

Fig. 3: FTLE^{-} for various time instances.

5. Conclusion

The main goal of this work was to reach a better understanding of LCSs and the ways of their identification. Data from a SPH simulation of free surface flow were used for FTLE analysis, which can visualize LCSs. The advantage of using SPH data is that they are naturally Lagrangian. The material approach analysis proved itself to be applicable and some characteristics of the flow were successfully identified. Many of the features of the flow, like the evolution of certain fluid parcels in time, would be impossible to find using only Eulerian flow field analysis tools.

In the future, it would be interesting to analyse different types of flows and use other tools for flow field analysis to see their capabilities and limits. Some attention should be also focused on improving the computational efficiency of the implementation.

Acknowledgements

This work was supported by the Grant Agency of the Czech Technical University in Prague, grant No. SGS20/112/OHK2/2T/12.

References

[1] J. Hunt, A. Wray, and P. Moin. ”Eddies, streams, and convergence zones in turbulent flows”. In: *Proceeding of the Summer Program in Center for Turbulence Research*, 1988, pp. 193-208.

[2] M. S. Chong, A. Perry, and B. Cantwell, ”A general classification of three-dimensional flow fields,” *Phys. Fluid Fluid Dynam.*, vol. 2, no. 5, pp 765-777, 1990. ISSN: 0899-8213. DOI: 10.1063/1.857730.

[3] J. Jeong and F. Hussain. ”On the identification of a vortex,” *J. Fluid Mech.*, vol. 285, pp. 69-94, 1995. ISSN: 0022-1120. DOI: 10.1017/S0022112095000462.

[4] G. Haller, ”An objective definition of a vortex,” *J. Fluid Mech.*, vol. 525, pp. 1-25, 2005. ISSN: 0022-1120. DOI: 10.1017/S0022112004002526.

[5] S. Shadden, F. Lekien, and J. Marsden, ”Definition and properties of Lagrangian coherent structures from finite-time Lyapunov exponents in two-dimensional aperiodic flows,”. In: *Physica D*, vol. 212, no.3, pp. 271-304, 2005. ISSN: 0167-2789. DOI: 10.1016/j.physd.2005.10.007.

[6] C. Conti, D. Rossinelli, P. Koumoutsakos. ”GPU and APU computations of Finite Time Lyapunov Exponent fields,”. *J. Comput. Phys.*, vol. 231, no. 5, pp. 2229-2244, 2012. ISSN: 0021-9991. DOI: 10.1016/j.jcp.2011.10.032.

[7] P. N. Sun, A. Colagrossi, S. Marrone, and A. M. Zhang. ”Detection of Lagrangian Coherent Structures in the SPH framework,” *Comput. Methods Appl. Mech. Eng.*, vol. 305, pp. 849-868, 2016. ISSN: 0045-7825. DOI: 10.1016/j.cma.2016.03.027.

[8] T. F Dauch, T. Rapp. G. Chaussonnet, S. Braun, M. C. Keller, J. Kaden, R. Koch, C. Dachsbacher, and H. J. Bauer. “Highly efficient computation of Finite-Time Lyapunov Exponents (FTLE) on GPUs based on three-dimensional SPH datasets,” *Comput. Fluids*, vol. 175, pp. 129-141, 2018. ISSN: 0045-7930. DOI: 10.1016/j.compfluid.2018.07.015.

[9] G. R. Liu and M. B. Liu. *Smoothed particle hydrodynamics - A meshfree particle method*. New Jersey, NJ: World Scientific, 2003.ISBN: 9789812564405.

[10] J. J. Monaghan and R. A. Gingold. “Shock simulation by the particle method SPH,” *J. Comput. Phys.*, vol. 52, no. 2, pp. 374-389, 1983. ISSN: 0021-9991. DOI: 10.1016/0021-9991(83)90036-0.

[11] S. Adami, X. Y. Hu, and N. A. Adams. “A generalized wall boundary condition for smoothed particle hydrodynamics,”. *J. Comput. Phys.*, vol. 231, no. 21, pp. 7057-7075, 2012. ISSN: 0021-9991. DOI: 10.1016/j.jp.2012.05.005.

[12] P. Jančík and T. Hyhlík. “Pressure evaluation during dam break using weakly compressible SPH,”. In: *Experimental Fluid Mechanics 2018*, Liberec, 2018, pp. 219-224.

[13] P. Jančík and T. Hyhlík. “Forces on vertical walls after dam break using weakly compressible SPH method,” *AIP Conf. Proc.*, vol. 2118, no.1, pp. 30018, 2019. ISSN: 0094-243X. DOI: 10.1063/1.5114746.